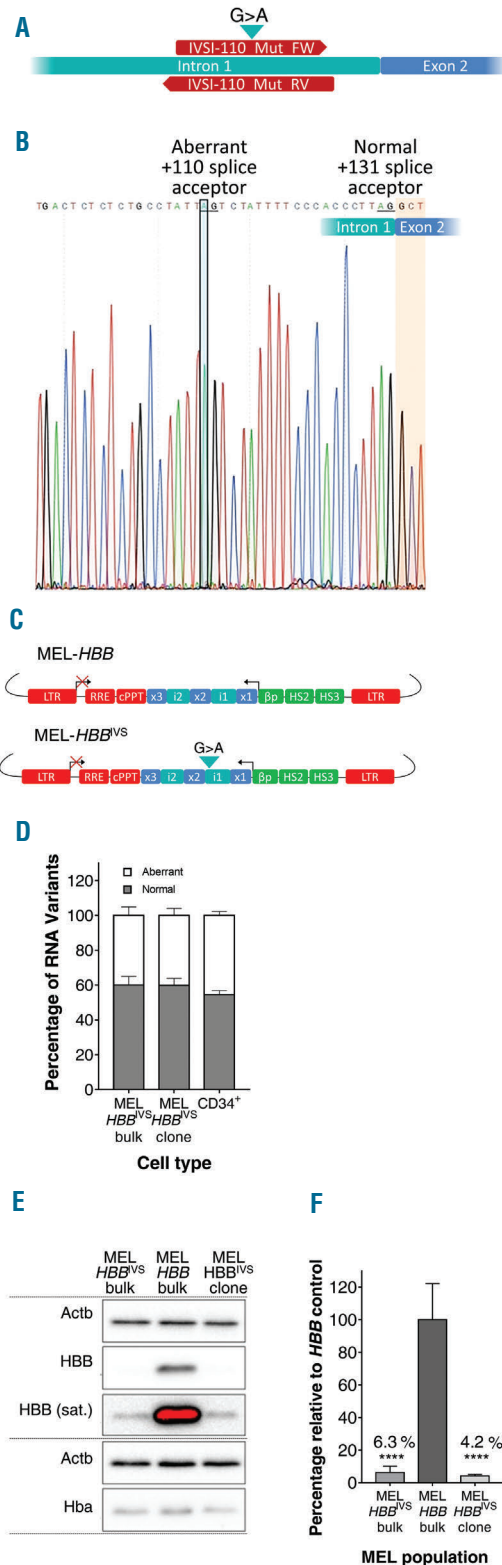


## Short-hairpin RNA against aberrant $HBB^{IVS1-110(G>A)}$ mRNA restores $\beta$ -globin levels in a novel cell model and acts as mono- and combination therapy for $\beta$ -thalassemia in primary hematopoietic stem cells

The hemoglobinopathy  $\beta$ -thalassemia is a common and potentially lethal monogenic disease characterized by deficient  $\beta$ -globin production. Standard palliative

treatment comprises regular blood transfusions and iron chelation therapy. The only widely applied cure is transplantation of allogeneic hematopoietic stem and progenitor cells, which often suffers from immunological complications and is available only to few patients. Efficiency of alternative correction by gene therapy is determined by underlying mutations, calling for its stratified application.<sup>1</sup> The severe  $HBB^{IVS1-110(G>A)}$  splicing mutation is common in many countries (Online Supplementary Figure S1),<sup>2</sup>



**Figure 1. Creation and characterization of humanized MEL cell lines.** A. Circular amplification of the intron1-exon2 border of the *GLOBE* transfer vector with mutagenic primers IVSI-110\_Mut\_FW and IVSI-110\_Mut\_RV to produce a mutated amplicon for production of *GLOBE*<sup>IVS1-110(G>A)</sup>. B. Sequence confirmation of mutagenesis for bacterial clones of the final *GLOBE*<sup>IVS1-110(G>A)</sup> plasmid across the intron1-exon2 border. C. The provirus forms of *GLOBE* and *GLOBE*<sup>IVS1-110(G>A)</sup> as held in the novel humanized cell lines MEL-*HBB* and MEL-*HBB*<sup>IVS</sup>, respectively. Green: core sequences for hypersensitive sites (HS2, HS3) of the  $\beta$ -globin locus control region and the human *HBB* promoter ( $\beta$ p) as human control elements of *HBB* expression; Purple: exons ("x") and introns ("i") of *HBB*; Red: Rev response element (RRE), central polypurine tract (cPPT) and transcriptionally inactivated long terminal repeat (LTR) as viral control elements; Black arrows: transcription from the provirus. D. Relative abundance of aberrant and normal *HBB* RNA in bulk MEL-*HBB*<sup>IVS</sup> (VCN 1.9) and clonal MEL-*HBB*<sup>IVS</sup> (VCN 1) compared to *HBB*<sup>IVS1-110(G>A)</sup>-homozygous CD34<sup>+</sup> cells. E. Representative immunoblot showing same-gel, same-membrane Actb and *HBB* expression and same-gel, same-membrane Actb and Hba expression, as indicated by dashed horizontal lines, including saturated exposure (HBB (sat.)) to visualize HBB bands for MEL-*HBB*<sup>IVS</sup> cell lines; red color indicates saturation. F. HBB band intensities for immunoblots of independent transductions (n=3) normalized for Hba expression and displayed as a percentage of average expression for MEL-*HBB* (arithmetic mean  $\pm$  sample standard deviation). Results of group-wise comparison of MEL-*HBB*<sup>IVS</sup> cell lines compared to MEL-*HBB* control by one-way ANOVA with Dunnett's multiple comparison test: \*\*\*\**P*<0.0001 (calculation threshold).

results in a 90% reduction of HBB ( $\beta$ -globin) and creates aberrant mRNA containing a 19-nt intronic fragment with an in-frame stop codon. Although potent targets of nonsense-mediated decay (NMD), aberrant  $HBB^{IVS1-110(G>A)}$  transcripts are abundant in erythroid cells of homozygous patients and disease models,<sup>3,4</sup> possibly owing to saturation of NMD by high substrate levels.<sup>5</sup> According to still limited data from preclinical studies and clinical trials,  $HBB^{IVS1-110(G>A)}$  appears recalcitrant to therapy by gene addition compared to other  $HBB$  mutations, suggesting aberrant transcripts as pathological *trans* factors likely acting by co-translational inhibition.<sup>6,7</sup> Their reduction by oligonucleotide-mediated splice correction may never reach therapeutic efficiency and would require chronic application,<sup>4</sup> whereas lentiviral delivery of short-hairpin

(sh)RNAs is robust and potentially translatable for curative  $\beta$ -thalassemia therapy.<sup>8</sup>

Here, we evaluate shRNA-mediated therapy of  $HBB^{IVS1-110(G>A)}$  thalassemia, firstly in a novel murine erythroleukemia (MEL) cell line encoding a human  $HBB^{IVS1-110(G>A)}$  transgene (MEL- $HBB^{IVS}$ ), and secondly in  $HBB^{IVS1-110(G>A)}$ -homozygous CD34<sup>+</sup> cells, either as monotherapy or after transduction with the *GLOBE HBB* gene-addition vector (see *Online Supplementary Methods* and *Supplementary Table S4* for all experimental procedures). Humanized MEL- $HBB^{IVS}$  cells and MEL- $HBB$  normal controls were created by lentiviral transduction (Figure 1A–C). After determination of vector copy number per cell (VCN),<sup>9</sup> bulk populations (MEL- $HBB^{IVS}$  at VCN 1.9 and MEL- $HBB$  at VCN 2.0) and a clonal cell line

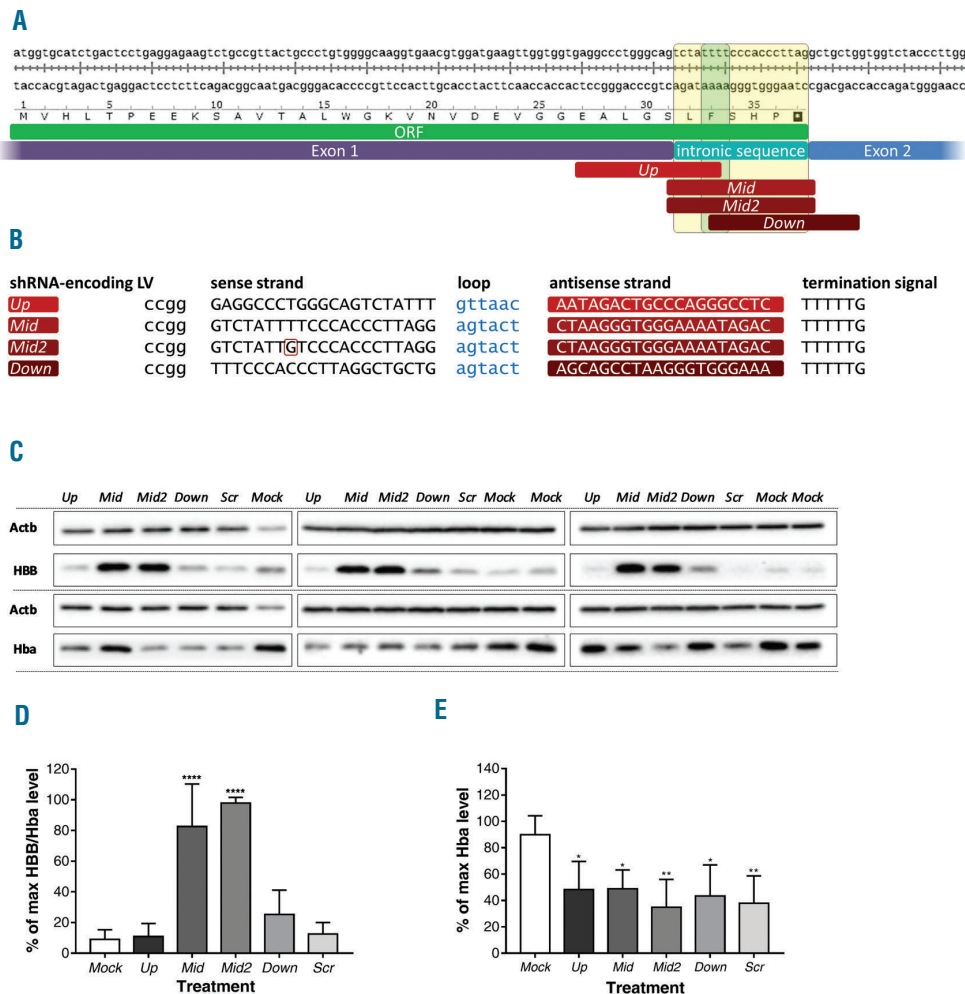


**Figure 2. Target sequences of  $HBB^{IVS1-110(G>A)}$ -specific shRNAs and functional analysis in humanized MEL cells.** A. Double-stranded cDNA sequence of the main  $HBB^{IVS1-110(G>A)}$ -derived transcript, with a stop codon (\*) in the aberrantly retained 19-nt intronic sequence including the open reading frame (ORF). Target sequences for four  $HBB^{IVS1-110(G>A)}$ -specific shRNAs, *Up*, *Mid*, *Mid2* and *Down*, are indicated relative to the 19-nt intronic sequence (yellow overlay) and its central dT<sub>4</sub> sequence (green overlay). B. Complete shRNA-encoding DNA sequence for all four  $HBB^{IVS1-110(G>A)}$ -specific shRNAs, excluding flanking nucleotides for cloning into pLKO.1. Rounded rectangle: mismatched nucleotide in the *Mid2* sense strand, breaking up the dT<sub>4</sub> sequence. C. Immunoblots for MEL- $HBB^{IVS}$  cells collected at day 6 of differentiation for three independent experiments (n=3). Actb, Hba: endogenous  $\beta$ -actin and  $\alpha$ -globin, respectively; HBB: human  $HBB^{IVS}$ -transgene-derived  $\beta$ -globin. Dashed lines separate same-gel and -membrane analyses derived from the same experiment. For raw volume measurements of band intensities, see *Online Supplementary Figure S3*. D. Percentage of differentiation-normalized HBB chain levels relative to the highest value for each experiment, as extracted from C; Significant results for group-wise comparisons vs. *Mock*: *Mid* or *Mid2* \*\*\*\* $P$ <0.0001 (calculation threshold). E. Percentage of Actb-normalized Hba levels relative to the highest value for each experiment, as extracted from C; Significant results for group-wise comparisons vs. *Mock*: *Up* \* $P$ =0.0359, *Mid* \* $P$ =0.0381, *Mid2* \*\* $P$ =0.0056, *Down* \* $P$ =0.0183, *Scr* \*\* $P$ =0.0086; *Mock*: *Mock* treatment without vector; *Scr*: treatment with vector encoding a scrambled shRNA, other column and lane labels specify LV-encoded shRNAs. *P* values reported are for group-wise comparison by one-way ANOVA with Dunnett's multiple comparison test. Bar charts show arithmetic mean  $\pm$  sample standard deviation.

(MEL-*HBB*<sup>IVS</sup> at VCN 1) were used for further experimentation. MEL-*HBB*<sup>IVS</sup> and MEL-*HBB* faithfully represented *HBB*<sup>IVS1-110(G>A)</sup>-derived transcript expression ratios (40% aberrant mRNA compared with 46% in *HBB*<sup>IVS1-110(G>A)</sup>-homozygous CD34<sup>+</sup>) and mutation-specific reduction in HBB expression (MEL-*HBB*<sup>IVS</sup> showing 6.3% of MEL-*HBB* human HBB levels)(Figure 1E and F).<sup>3</sup> Accordingly, gene-dosage equivalent expression of mutant and normal transgenes in bulk MEL-*HBB*<sup>IVS</sup> (VCN 1.9) and MEL-*HBB* (VCN 2.0) cells, respectively, suggested a HBB protein ratio of 15.8 for normal compared to mutant. We thus regarded a 15.8-fold HBB induction after treatment as target level for correction in this model.

In order to reduce aberrant *HBB*<sup>IVS1-110(G>A)</sup> mRNA and its potential interference with HBB expression, we designed

shRNAs targeting the aberrant-specific 19-nt mRNA sequence (Figure 2A). For proof of principle and in order to achieve saturating shRNA expression and effect, we employed the pLKO.1 lentiviral vector (LV)<sup>10</sup> with its constitutive RNA-polymerase-III (RNAPolIII)-dependent U6 promoter at high multiplicity of infection (MOI). Of the four *HBB*<sup>IVS1-110(G>A)</sup>-specific shRNAs designed, two avoided full inclusion of a potential RNAPolIII terminator, a dT<sub>4</sub> run central to the 19-nt sequence.<sup>11</sup> To this end, one of the shRNA targets had overlap upstream (*Up*), the other overlap downstream (*Down*) with the dT<sub>4</sub> sequence. A third, central target comprising the full 19-nt sequence was represented by two shRNAs, one with perfect complementarity and loop structure (*Mid*), the other with a mutated dT<sub>4</sub> sequence (TTGT) in its passenger strand (*Mid2*)(Figure 2B).

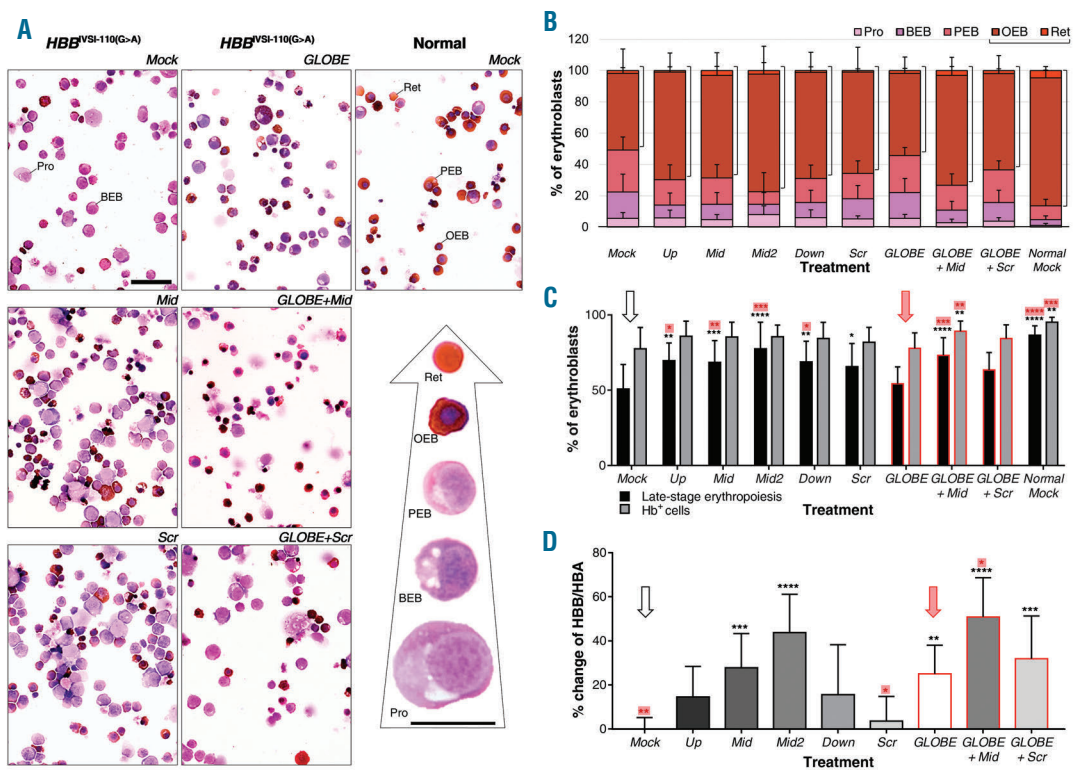


**Figure 3. Functional correction of primary *HBB*<sup>IVS1-110(G>A)</sup>-homozygous CD34<sup>+</sup> cells.** Data from independent cultures representing four different *HBB*<sup>IVS1-110(G>A)</sup>-homozygous patients (n=12 for Mock, n=10 for *Mid* and Scr, n=6 for *Up*, *Down* and each combination with GLOBE, n=5 for *Mid2*) for relative HBB levels, erythroid differentiation and hemoglobinization, scored 7 days after transduction. A. Representative microscopy images of cyto-centrifuged histologically stained samples (scale bar 20  $\mu$ m) and enlarged reference images of observed erythroid-lineage differentiation (scale bar 10  $\mu$ m). Genotypes (in bold) and treatments (in italics) are indicated. B. Percentage of erythroid subpopulations across all experiments according to differential counting of cells (Mock n=4079, *Up* n=777, *Mid* n=2210, *Mid2* n=452, *Down* n=724, Scr n=3346, GLOBE n=2873, GLOBE+*Mid* n=1695, GLOBE+Scr n=2051 and mock-treated normal samples n=847), with brackets combining phases for late-stage erythroid differentiation (orthochromatophilic erythroblasts, reticulocytes). C. Differential counting for late-stage erythropoiesis (black bars) and dianisidine-positive, hemoglobinized cells (grey bars), analyzed by Kruskal-Wallis test with Dunn's multiple comparisons test. The tests were applied twice independently, once against Mock and once against GLOBE, as indicated by an arrow for the respective reference treatment and asterisks in corresponding color and shading for significantly different test samples. Mock vs.: *Up* \*\**P*=0.002046, *Mid* \*\*\**P*=0.0007217, *Mid2* \*\*\*\**P*<9.0 $\times$ 10<sup>-5</sup>, *Down* \*\**P*=0.005604, Scr \**P*=0.01415, GLOBE+*Mid* \*\*\*\**P*<3.2 $\times$ 10<sup>-5</sup>, \*\**P*=0.006459, Normal \*\*\*\**P*<2.3 $\times$ 10<sup>-5</sup>, \*\*\**P*=0.001298; GLOBE vs.: *Up* \**P*=0.1334, *Mid* \*\**P*=0.009452, *Mid2* \*\*\**P*=0.0001369, *Down* \**P*=0.02607, GLOBE+*Mid* \*\*\*\**P*=0.0005801, \*\**P*=0.004081, Normal Mock \*\*\*\**P*=1.4 $\times$ 10<sup>-5</sup>, \*\*\**P*=0.0007011. D. HPLC results for the percentage change of HBB/HBA ratios, compared with Mock, analyzed by one-way ANOVA with Dunnett's multiple comparison test. The tests were applied twice independently, once against Mock and once against GLOBE, as indicated by an arrow for the respective reference treatment and asterisks in corresponding color and shading for significantly different test samples. Mock vs.: *Mid* \*\*\**P*=0.0004, *Mid2* \*\*\*\**P*<0.0001, GLOBE \*\**P*=0.0085, GLOBE+*Mid* \*\*\*\**P*<0.0001, GLOBE+Scr \*\*\**P*=0.0005; GLOBE vs.: Mock \*\**P*=0.0085, Scr \**P*=0.0419, GLOBE+*Mid* \*\**P*=0.0243. Red outlines: transduction with GLOBE and time-shifted co-transduction with shRNA-encoding vectors; Corresponding percentage changes for additional  $\beta$ -like globin chains and combinations and approximate  $\beta$ -like globin chain distribution for each treatment are shown in Online Supplementary Figure S4. Corresponding differentiation-corrected HBB expression levels, including additional cultured samples from normal donors, are shown in Online Supplementary Figure S5. Normal: healthy control sample; Mock: mock treatment without vector; Scr: treatment with vector encoding a scrambled shRNA; other column and lane labels specify LVs; Pro: proerythroblast; BEB: basophilic erythroblast; PEB: polychromatophilic erythroblast; OEB: orthochromatophilic erythroblast; Ret: reticulocyte.

All four shRNAs plus scrambled control shRNA (*Up*, *Mid*, *Mid2*, *Down*, *Scr*) were then transduced individually into MEL-*HBB*<sup>IVS1-110(G>A)</sup> VCN-1 cells and compared with mock-transduced (*Mock*) controls. Functional correction of transduced cells was analyzed by immunoblots for detection of *HBB*<sup>IVS1-110(G>A)</sup>-derived HBB at day 6 of differentiation, which consistently showed unchanged expression for *Up* and a two-fold, yet statistically insignificant, change of expression for *Down*. Importantly, HBB expression increased significantly for *Mid* and *Mid2*, from (9.1±6.3)% of maximum Hba ( $\alpha$ -globin)-normalized band intensity for the mock-treated sample, to (82.6±27.7)% for *Mid* and (97.8±3.7)% for *Mid2* (Figure 2C and 2D). Compared with the HBB protein ratio of 15.8 between MEL-*HBB* and MEL-*HBB*<sup>IVS</sup> cells as an approximate target level for correction, shRNAs alone induced HBB expression compared to *Mock* 9.1-fold (58%) for *Mid* and 10.8-fold (69%) for *Mid2*. Same-sample analyses of corresponding *HBB* mRNA expression showed by contrast that *Down*, but none of the other shRNAs, significantly upregulated the ratio of normal to aberrant *HBB* mRNA compared to *Mock* (Online Supplementary Figure S2A). For total (normal+aberrant) *HBB* mRNA levels, no significant differences were detected at considerable variation between experiments (Online Supplementary Figure S2B). Notably, immunoblots also indicated reduced Actb-normalized Hba expression and thus reduced MEL-*HBB*<sup>IVS</sup> differentiation after shRNA treatment (Figure 2E). This phenomenon is likely related to toxicity from high VCNs and unregulated shRNA expression.<sup>12</sup>

For evaluation of therapeutic activity in clinically relevant cells, *Up*, *Mid*, *Mid2*, *Down*, *Scr* and the *GLOBE* gene-addition vector were then also applied as lentiviral monotherapy to primary *HBB*<sup>IVS1-110(G>A)</sup>-homozygous CD34<sup>+</sup> cells in culture and compared with *Mock*.<sup>13</sup> Additionally, combination treatments of *GLOBE* with *Mid* (to exemplify both superior, central *Mid* and *Mid2*, shRNAs) and with *Scr* were performed. As a first key parameter of  $\beta$ -thalassemia pathology, erythroid differentiation was analyzed by cyto centrifugation, cell staining and treatment-blinded microscopic analysis (exemplified in Figure 3A). These analyses revealed significantly increased late-erythroid differentiation, scored as presence of orthochromatophilic erythroblasts and reticulocytes, after shRNA treatment, from 50.7% for *Mock* toward the 86.5% observed for normal controls (Figure 3B). All *HBB*<sup>IVS1-110(G>A)</sup>-specific shRNAs and *GLOBE+Mid* gave significant increases over *Mock* (Figure 3C, black bars), with lower-level induction also by *Scr*, possibly owing to stress-induced erythropoiesis and HBB expression.<sup>14</sup> Of note, at VCN 3.2±1.6, *GLOBE* monotherapy did not achieve significant correction of erythroid differentiation in *HBB*<sup>IVS1-110(G>A)</sup>-homozygous samples, and *GLOBE+Mid* significantly outperformed *GLOBE* alone. Complementary microscopic scoring of hemoglobinization as separate measurement revealed that only the *GLOBE+Mid* combination treatment significantly increased hemoglobinization compared with *Mock* and *GLOBE* (Figure 3C, grey bars). As a second key parameter of  $\beta$ -thalassemia pathology, the ratio of  $\beta$ -globin to  $\alpha$ -globin expression (HBB/HBA) was analyzed for transduced *HBB*<sup>IVS1-110(G>A)</sup>-homozygous samples by reversed-phase high-performance liquid chromatography (HPLC), with the results matching those for the parameter of erythroid differentiation. Specifically, comparison of HBB/HBA with *Mock* showed significant increases for *GLOBE+Mid* by (50.81±17.85)%, *Mid2* by (43.72±17.45)%, *Mid* by (27.72±15.61)%, *GLOBE+Scr* by (31.92±19.39)% and

*GLOBE* by (25.00±13.01)% (in order of ascending *P* values, Figure 3D). Compared with *GLOBE*, HBB/HBA was significantly decreased for *Mock* and *Scr*, and was significantly increased for *GLOBE+Mid*. Total  $\beta$ -like globin chains varied considerably between experiments and were increased for all treatments, most highly for *Mid2* by (42.57±23.56)% and *GLOBE+Mid* by (38.89±32.05%)(Online Supplementary Figure S4). Against high baseline levels of raw HBB/HBA ratios in culture (0.58 for *Mock* against 1.03 for Normal controls), *Mid2* and *GLOBE+Mid* were the most effective treatments, reaching ratios of 0.82 and 0.79, respectively (Online Supplementary Figure S5). Of note, whereas *GLOBE+Mid* compared with *GLOBE* alone significantly improved late-erythroid differentiation, hemoglobinization and HBB/HBA protein ratios, *GLOBE+Mid* compared with *Mid* alone resulted in only slight and statistically insignificant increases.

Overall, shRNA-encoding IVs gave high VCNs with no consistent further HBB increases above VCN 5 for *Mid* and *Mid2* and with marked cell death after transduction (Online Supplementary Figures S6 and S7), both in all likelihood because of efficient transduction with the comparably small shRNA-expressing IVs.<sup>12</sup> For normal CD34<sup>+</sup> samples (n=2), *Up*, *Mid* and *Mid2* gave variably increased HBB/HBA protein ratios, whereas *Down* reduced HBB/HBA (Online Supplementary Figure S8), a preliminary finding revealing that *Mid* and *Mid2* do not interfere with HBB expression from normal loci.

This study establishes aberrant *HBB*<sup>IVS1-110(G>A)</sup> mRNA as a partially dominant causative agent of disease severity in *HBB*<sup>IVS1-110(G>A)</sup> thalassemia and as a potent target for mutation-specific gene therapy. High titers of shRNA-encoding vectors and constitutive expression were applied, whereas for potential clinical translation, moderate VCN and erythroid-specific shRNA expression will be required.<sup>3</sup> The specific mechanism of shRNA-mediated HBB induction is under investigation, with findings in MEL-*HBB*<sup>IVS</sup> cells for *HBB* RNA and protein levels, and in CD34<sup>+</sup> cells for HBB protein levels suggesting differential modes of action for *Down* compared with *Mid* and *Mid2* shRNAs (see Online Supplementary Discussion). In comparison with LV *HBB* addition and at levels of correction in *HBB*<sup>IVS1-110(G>A)</sup>-homozygous CD34<sup>+</sup> cells similar to or higher than those for *GLOBE*, application of the smaller shRNA-encoding vectors offers up to ten-fold higher vector yield (Online Supplementary Table S2) and may thus give more patients access to treatment. Beyond *HBB*<sup>IVS1-110(G>A)</sup> and many similar thalassemia-causing mutations (see IthaGenes)<sup>2</sup> with splice defects, hundreds of genetic diseases (see DBASS3/5)<sup>15</sup> are associated with aberrant transcripts, whose stability and causative role in disease pathology mostly remain to be investigated. The novel approach of shRNA treatment against aberrant mRNA is thus potentially suitable for a range of disorders. Here, it proved effective as monotherapy in primary *HBB*<sup>IVS1-110(G>A)</sup>-homozygous CD34<sup>+</sup> cells in culture, and in combination treatment significantly improved upon gene therapy by *HBB* addition.

Petros Patsali,<sup>1,2</sup> Panayiota Papasavva,<sup>1,3</sup>  
Coralea Stephanou,<sup>1,2</sup> Soteroulla Christou,<sup>4</sup> Maria Sitarou,<sup>4</sup>  
Michael N. Antoniou,<sup>2</sup> Carsten W. Lederer,<sup>1,3,†,\*</sup> and  
Marina Kleanthous<sup>1,3,†</sup>

<sup>1</sup>Department of Molecular Genetics Thalassemia, The Cyprus Institute of Neurology and Genetics, Nicosia, Cyprus; <sup>2</sup>Department of Medical and Molecular Genetics, King's College London, UK; <sup>3</sup>Cyprus School of Molecular Medicine, Nicosia, Cyprus and <sup>4</sup>Thalassemia Centre, Ministry of Health, Cyprus

†Shared last authors

*Acknowledgments: we are indebted to our blood donors, without whom this work would not have been possible. We thank Aglaia Athanasiadou for encouraging our investigation of mutation-specific gene therapy.*

*Funding: The present study was co-funded by the European Union's Seventh Framework Program for Research, Technological Development and Demonstration under grant agreement no. 306201 (THALAMOSS), and by the Republic of Cyprus through the Research Promotion Foundation under grant agreement YTEIA/BIOΣ/0311(BE)/20 and through core funding of The Cyprus Institute of Neurology and Genetics.*

*Correspondence: lederer@cimg.ac.cy  
doi:10.3324/haematol.2018.189357*

*Information on authorship, contributions, and financial & other disclosures was provided by the authors and is available with the online version of this article at [www.haematologica.org](http://www.haematologica.org).*

## References

- Breda L, Casu C, Gardenghi S, et al. Therapeutic hemoglobin levels after gene transfer in  $\beta$ -thalassemia mice and in hematopoietic cells of  $\beta$ -thalassemia and sickle cells disease patients. *PLoS One*. 2012; 7(3):e32345.
- Kountouris P, Lederer CW, Fanis P, Feleki X, Old J, Kleanthous M. IthaGenes: An interactive database for haemoglobin variations and epidemiology. *PLoS One*. 2014;9(7):e103020.
- Vadolas J, Nefedov M, Wardan H, et al. Humanized  $\beta$ -thalassemia mouse model containing the common IVSI-110 splicing mutation. *J Biol Chem*. 2006;281(11):7399-7405.
- El-Beshlawy A, Mostafa A, Youssry I, et al. Correction of aberrant pre-mRNA splicing by antisense oligonucleotides in beta-thalassemia Egyptian patients with IVSI-110 mutation. *J Pediatr Hematol Oncol*. 2008;30(4):281-284.
- Paillusson A, Hirschi N, Vallan C, Azzalin CM, Mühlemann O. A GFP-based reporter system to monitor nonsense-mediated mRNA decay. *Nucleic Acids Res*. 2005;33(6):e54-e54.
- Breda L, Casu C, Casula L, et al. Following beta-globin gene transfer, the production of hemoglobin depends upon the beta-thalassemia genotype. *Blood*. 2009;114(22):978.
- Thompson AA, Walters MC, Kwiatkowski J, Rasko JEJ, Ribeil JA, Hongeng S, Magrin E, Schiller GJ, Payen E, Semeraro M, Moshous D, Lefrere F, Puy H, Bourget P, Magnani A, Caccavelli L, Diana JS, Suarez F, Monpoux F, Brousse V, Poirot C, Brouzes C, Meritet JF, Pondarré C, Beuzard Y, Chrétien S, Lefebvre T, Teachey DT, Anurathapan U, Ho PJ, von Kalle C, Kletzel M, Vichinsky E, Soni S, Veres G, Negre O, Ross RW, Davidson D, Petrusich A, Sandler L, Asmal M, Hermine O, DeMontalembert M, Hacein-Bey-Abina S, Blanche S, Leboulch P, Cavazzana M. Gene Therapy in Patients with Transfusion-Dependent  $\beta$ -Thalassemia. *N Engl J Med*. 2018; 19;378(16):1479-1493.
- Brendel C, Guda S, Renella R, et al. Lineage-specific BCL11A knock-down circumvents toxicities and reverses sickle phenotype. *J Clin Invest*. 2016;126(10):3868-3878.
- Christodoulou I, Patsali P, Stephanou C, Antoniou M, Kleanthous M, Lederer CW. Measurement of lentiviral vector titre and copy number by cross-species duplex quantitative PCR. *Gene Ther*. 2016; 23(1):113-118.
- Root DE, Hacohen N, Hahn WC, Lander ES, Sabatini DM. Genome-scale loss-of-function screening with a lentiviral RNAi library. *Nat Methods*. 2006;3(9):715-719.
- Arimbasseri AG, Rijal K, Maraia RJ. Transcription termination by the eukaryotic RNA polymerase III. *Biochim Biophys Acta*. 2013;1829(3-4):318-330.
- Manjunath N, Wu H, Subramanya S, Shankar P. Lentiviral delivery of short hairpin RNAs. *Adv Drug Deliv Rev*. 2009;61(9):732v745.
- Stephanou C, Papasavva P, Zachariou M, et al. Suitability of small diagnostic peripheral-blood samples for cell-therapy studies. *Cytotherapy*. 2017;19(2):311-326.
- Zheng Y, Miyamoto DT, Wittner BS, et al. Expression of  $\beta$ -globin by cancer cells promotes cell survival during blood-borne dissemination. *Nat Commun*. 2017;8:14344.
- Buratti E, Chivers M, Hwang G, Vorechovsky I. DBASS3 and DBASS5: databases of aberrant 3'- and 5'-splice sites. *Nucleic Acids Res* 2011;39(Database issue):D86-91.